# Current Status of Three Dimensional Growth Laws

**James A. Glazier**
**Burkhard Prause**
Department of Physics, 316 Nieuwland, University of Notre Dame, Notre Dame, IN 46556, USA

## Abstract

We review current theory, simulation and experiment for the growth of 3D bubbles in ideal dry froth. Theories assume either that the growth rate depends on bubble radius or topology. Radius based laws violate the Young-Laplace law. Topological theories can be either linear or non-linear in the number of faces ($f$). The growth law can hold either exactly for each bubble (as in 2D) or apply only to ensembles of bubbles with a given topology. Recent experiments suggest that the growth law is linear in $f$, but holds only for ensembles. We still lack both experimental and simulation results for possible growth laws depending on detailed topology or vertex number. Higher accuracy and better statistics are essential to resolve these issues.

## 1 Introduction

The growth rate of bubbles in a quasi-2D soap froth coarsening via diffusion is surprisingly simple. von Neumann's law states that the growth rate of a bubble is a linear function of its number of sides, is independent of its area and of the properties of its neighbors [1], inviting a mean field approach. The kinetics is separate from the topological of faces on side or bubble disappearance, which affects neighboring bubbles. This simplification has led to many mean field studies which treat the kinetics exactly and approximate the redistribution [2,3].

We do not yet know the rate of growth (or shrinkage) of a bubble in an ideal 3D dry foam growing by diffusive coarsening or on what variables it depends. Only recently have experiments and simulations measured the growth rates of individual bubbles [4-6]. Since the growth rate is fundamental to the evolution of cellular structures, its lack prevents the development of any adequate theory for 3D foams [3].

## 2 Curvature and Topology

In an ideal soap froth, minimisation of surface energy results in bubble faces that are minimal surfaces with constant mean curvature [7],

$$G \equiv 1/r_1 + 1/r_2, \tag{1}$$

where $r_1$ and $r_2$ are the two independent radii of curvature. The mean curvature determines the effective pressure difference across the grain wall, $\Delta P$, via the Young-Laplace relation [2],

$$\Delta P = \sigma(1/r_1 + 1/r_2), \tag{2}$$

where $\sigma$ is the surface tension. The rate of transfer of volume (and hence mass assuming that the material is effectively incompressible) across the boundary is proportional to the face area times the pressure difference, so the growth rate has the form:

$$\frac{\mathrm{d}V}{\mathrm{d}t} = \kappa \oiint_{surface} \vec{G} \bullet \mathrm{d}s, \tag{3}$$

where $\kappa$ is an effective diffusion constant and $\vec{G}$ is a vector normal to the surface in the convex direction with magnitude $G$. In polycrystals the local curvature determines the local boundary velocity:

$$v(\vec{r}) = \mu\vec{G}, \tag{4}$$

where $\mu$ is the boundary mobility. Clearly, any bubble that obeys eqns. (1) and (2) also obeys eqn. (4) [8,9]. Less obviously, a grain obeying eqn. (4) should have the same total growth rate as a bubble with the same shape. Since G scales inversely with the bubble radius, $r$, ($G \propto 1/r \propto V^{1/3}$) while the total surface area is proportional to $r^2$, the r.h.s. of eqn. (3) **must** be the product of the radius with a term depending on the shape. Combining all $V$ dependencies in the l.h.s. we obtain a growth law of the form:

$$\frac{\mathrm{d}V_f^{2/3}}{\mathrm{d}t} = \frac{1}{V_f^{1/3}}\frac{\mathrm{d}V_f}{\mathrm{d}t} = \kappa C(\text{Shape}). \tag{5}$$

Because the total volume is constant, the joint distribution of volume and shape constrains $C(\text{Shape})$, $0 = \sum_{\text{Shape}}\int \mathrm{d}V_f/\mathrm{d}t\ P(V,\text{Shape})\mathrm{d}V = \sum_{\text{Shape}}C(\text{Shape})V_{\text{Shape}}^{1/3}$, where $P$ is the probability of a bubble having a given shape and size.

The wall of a planar 2D bubble has only one radius of curvature so eqn. (3) depends only on the number of sides, **n**, of the grain, and the area $a_n$ of an $n$-sided bubble grows as [1], $\mathrm{d}a_n/\mathrm{d}t = k(n-6)$.

In 3D, a derivation analogous to that of von Neumann's law fails, because the topology determines not the mean, but the Gaussian curvature, $K \equiv (r_1 r_2)^{-1/2}$ [10]. $K$ and $G$ are independent so the growth rate need not depend on the topology. The relation (if any) between mean curvature and topology (whether on $f$ or on the exact distribution of edges, faces and vertices) for a minimal surface remains a major unsolved problem in classical geometry. Even an averaged growth law dependent on topology implies that the foam **is** imposing a relation between mean $G$ and mean $K$, otherwise the growth rate of a bubble would depend on the detailed local geometry and no growth law would exist at all.

## 3 Hypothetical Growth Laws and their Effect on Kinetic Exponent

Eqns. (1), (2) and (4) are inescapable for ideal foams but they can fail in real froths, *e.g.* if the bubbles are spherical and well separated and the liquid carries a substantial partial pressure of gas the Lifschitz-Slyozov law replaces the Young-Laplace law, eqn. (2), and the growth law becomes [11,12], $\mathrm{d}V(r)/\mathrm{d}t = \gamma\left(r(t)_C^{-1} - r^{-1}\right)$, where $r_c$ is a critical radius corresponding to the effective pressure in the continuous phase. In a **scaling state**, *i.e.* a configuration in which the

distributions of volumes and topologies remain constant, simple dimensional arguments show that the mean radius, $<r>$, must evolve as $<r> \propto t^{1/3}$ [13]. Measurements of the growth exponent in foams and metals agree that the scaling exponent is 1/2 rather than 1/3 [2,13-15]. Any law of the form of eqn. (5) gives the observed growth exponent of 1/2 [13].

The L.-S. law remains seductive because it is much simpler than eqn. (5) and seems to follow from the following argument. Bubbles with more faces have larger volume. Claimed forms of this relation differ, but the consensus is (fig. 1) [6,16]:

$$<V_f> \propto f^3. \tag{6}$$

If we substitute $V^{1/3}$, *i.e.*, $r$, for $f$ and neglect to notice that the two sides of eqn. (6) are dimensionally different we then must omit the required prefactor of $r$ in eqn. (5) to obtain a law of L.-S. form. Even today papers appear simulating close packed coarsening with the L.-S. law rather than eqn. (5) [17-19]. Rivier proposed [20], $\left[ dV_f / dt \right] = \kappa \left( f - \langle f \rangle \right)$, where $<f>$ is the average number of faces in the froth and the [ ] average is over all grains in a topological class that do not change their number of faces during the brief interval $dt$, giving a growth law, $<r> \propto t^{1/3}$, and not conserving total volume.
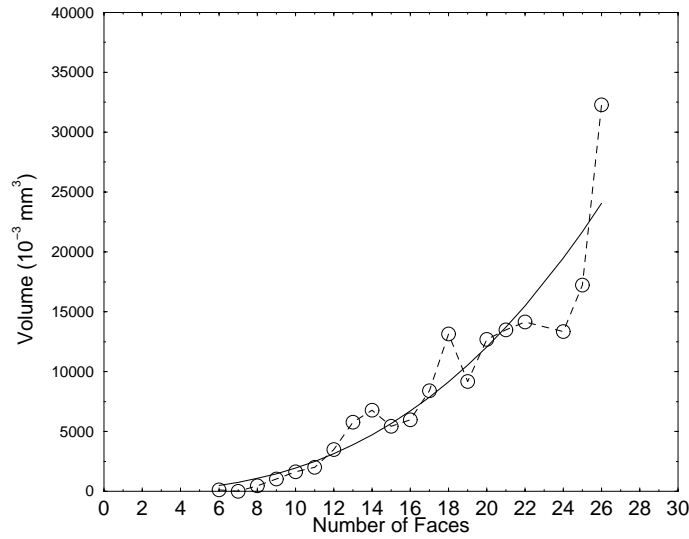


Figure 1. The relation between a bubble's volume and its number of faces. The average volumes of bubbles with $f$ faces are plotted versus $f$. MRI experiment on gelatine foam.

## 4 Symmetrical Bubble Theories

By assuming simplified bubble shapes, we can estimate the geometrical factor $C(f)$ in eqn. (5), though we cannot say whether the growth rate is exact for $f$-faced bubbles. A typical $C(f)$ is non-linear, lying below the linear fit for very small or large $f$, *i.e.* outside the typical experimental range for real foams.

Fortes assumed that all edges of a face lie in a plane and that all faces are regular polyhedra with $n=6-12/f$ sides [21] and that the velocity of edges or vertices was independent of bubbles size, leading to $<r> \propto t$ growth kinetics with zero growth for $f=13.4$ faces (fig. 2a). Mullins assumed that the vertices of each face lay in a plane, and that all faces are pentagonal [8] (fig.

2a). His equation gives zero growth for *f=13.3*. These models do not conserve total volume for arbitrary volume and topology distributions. Sire, assuming that faces are planar and regular, but allowing each face to have a different number of sides, attained a similar result depending on the assumed relation between number of sides and area for faces [22].
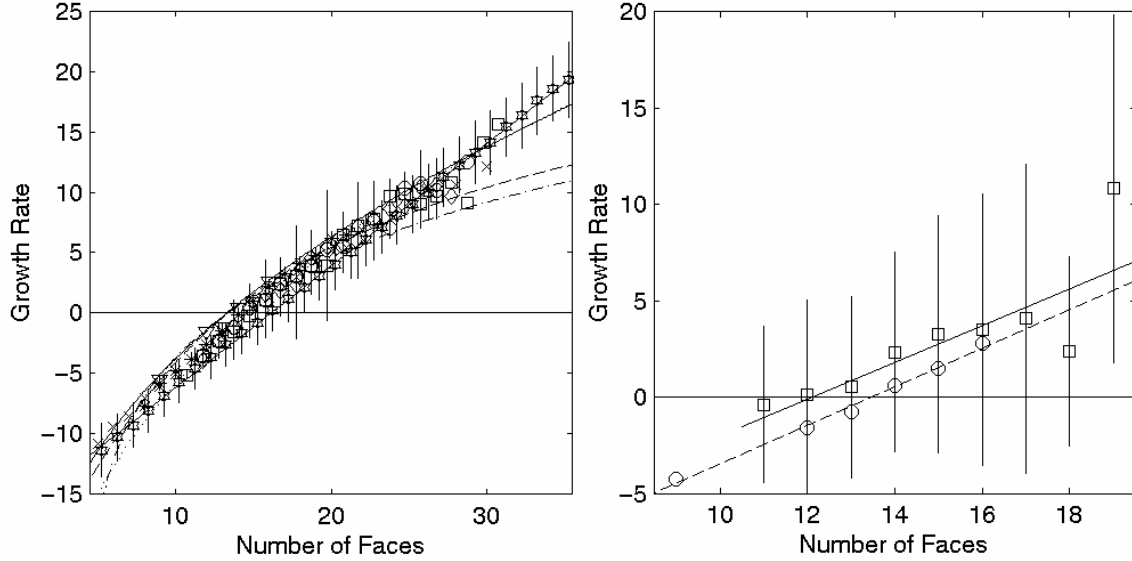


Figure 2a. Growth rates as a function of number of faces for Fortes' edge and vertex models (Dashed lines), Mullins' model (Solid Line), Kawasaki's vertex model (Squares, Circles and Diamonds), Weygand's vertex model (Dotted Line), Monnereau *et al.*'s boundary dynamics model (Triangles), Wakai's boundary dynamics model (Xs and Stars) and Glazier's Potts model (Star of David). 2b. Monnereau *et al.*'s optical tomography experiments (Circles) and our MRI experiments (Squares).

## 5 Simulations

### 5.1 Potts Model

Glazier simulated regular coarsening using the zero temperature *Q*-state Potts model on a third neighbor cubic lattice [9], originally introduced by Anderson, Grest and Srolovitz [23-25]. The Potts model results are difficult to interpret because the square lattice is highly non-Euclidean for small domains. Thus small domains shrink more rapidly than large domains, which increases the mean shrinkage rate for few-faced domains, which tend to be small. In addition, very small domains tend to shift their number of sides rapidly and be discarded from the calculation, creating a selection bias which makes very-few-faced grains shrink more slowly than expected. Correcting these artefacts results in a linear growth relation in the scaling state for $4 \leq f \leq 55$ (fig. 2a):

$$C(f) = f - f_0. \tag{7}$$

Glazier also showed that the growth rate for *f*-faced domains was independent of their size [9]. Later, Weaire and Glazier showed that volume conservation, eqn. (6), requires [26]:

$$f_0 = \langle f^2 \rangle / \langle f \rangle^2 , \tag{8}$$

provided eqn. (6) holds. The standard deviation of the growth rates is independent of the number of faces suggesting that the detailed topology is not important.

4

## 5.2 Vertex Models

Fuchizaki and Kawasaki have developed an elaborate vertex model derived from eqn. (4) [27]. Unlike their earlier models, they include points at the center of faces, to triangulate, making the result more like a boundary-dynamics simulation. They find good agreement with the linear form of eqn. (7) with $f_0$=15 (fig. 2a). Weygand *et al.* have implemented a model with the same basis with fewer approximations [28]. Strangely, they find a strongly nonlinear growth law with an emperical form (fig. 2a):

$$C(f) = -50 + 20.5 f^{1/3} , \qquad (9)$$

with zero growth for *f*=15.

## 5.3 Surface Evolver (Boundary Dynamics) Models

Surface Evolver is a software package that approximates minimal surfaces by triangulations of variable density. From the triangulation we can estimate the local curvature and hence implement eqn. (4) directly. Monnereau *et al.* used S.E. to simulate the growth of 28 domains (starting from a digitzed experiment) and obtained a linear growth law with $f_0$=13.8±0.2 [29] (fig. 2a). This result tracked 28 bubbles over a volume change of about 25 for $9 \leq f \leq 17$. Wakai *et al.* also used S.E. to simulate 3D coarsening beginning with 1000 domains (fig. 2a) [16]. Eqn. (7) with $f_0$=14.8 agrees well with their values for $C(f)$. S.E. should give a nearly perfect solution to eqn. (4) for fine triangulations and so should be able to distinguish whether the growth law holds for each bubble individually. Unfortunately neither paper gives the ranges of growth rates within topological categories or examines the dependence of grain growth on detailed topology. However, the results suggest that only the averaged law holds.

# 6 Experiments

## 6.1 Optical Techniques

Because foams are highly dispersive they are hard to see into. Reconstruction 3D structures is also tricky and time consuming. Nevertheless, studies of bubble sizes by optical stereography go back to the 1930s [30-33]. Others looked at the surface bubbles in the foam [18,34], which rules out calculations of topologies.

The first real optical tomography showed that the technique was practical, but made no quantitative measurements [35-37]. Monnereau *et al.* used optical tomography to reconstruct the topology of an experimental nitrogen foam semi-automatically, using S.E. to reconstruct the face contours, giving a very accurate estimate of bubble volumes, taking 28 slices through a dry liquid soap foam [4,5], each scan taking 45 seconds. They tracked to 28 bubbles over 9 hours, representing about a 25% volume change. They found a linear growth law for *f*=9, 11-16, with $f_0$=13.3±0.1, but could not determine whether the growth law was exact (fig. 2b).

## 6.2 Magnetic Resonance Imaging

Magnetic Resonance Imaging (MRI) is one of the few methods, which provides complete, non-invasive information about bubbles deep inside a foam. MRI of foam is difficult due to the small amount of liquid inside the sample volume, and the very large interfacial areas between liquid and gas, which tend to distort images and reduce the signal. We need both

spatial resolution better than the size of the Plateau borders and relatively fast acquisitions, since the foam coarsens while the image is being acquired.

The first 2D MRI images of foam measured the water content inside a column of liquid foam over time [38,39]. Gonatas *et al.* imaged 2D slices at fifty minutes per slice, measuring the bubble size distributions for bubbles as small as 250 $\mu$m over three days [40].

Unfortunately, ordinary soap froth is almost impossible to image. We optimized the magnetic properties of the foam, using $DyCl_3(TTHA)$ to avoid susceptibility artifacts and $CuSO_4$ to achieve fast magnetization relaxation, necessary for fast imaging. To slow coarsening and drainage and prevent wall breakage, we foamed a highly purified gelatin-water mixture with SDS as a surfactant. To reduce gravitational drainage and wall breakage, we cooled the foam to $281^\circ K \pm 0.1^\circ K$, maximizing its viscosity just above its freezing point. Samples prepared in this manner coarsened for six days before solidifying.



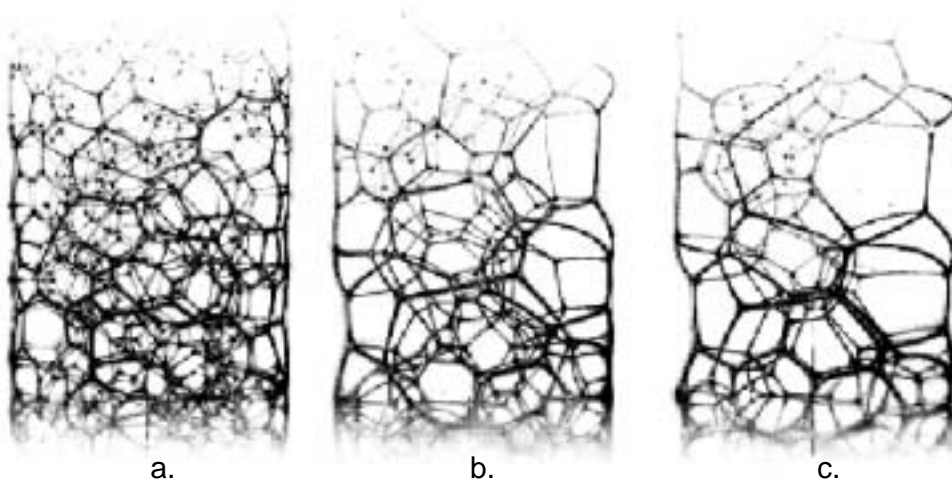a.                             b.                             c.

Figure 3. Maximum intensity projections of three-dimensional MRI reconstructions of a foam at three stages of development (a) = 24 hrs. (b) = 36 hrs. (c) = 48 hrs.

We imaged the foams in 3D, using our Bruker 300 MHz (7 Tesla) imaging spectrometer with high field gradients (96 G/cm). We resolved 256 x 128 x 128 voxels of side length 100 - 150 $\mu$m in about 14 minutes, using a 3D spin echo sequence with two to eight averages. A "snapshot" of the foam took 30 minutes initially and 120 minutes at the end (fig. 3).

To remove imaging artifacts and random noise from the reconstructed 3D image we threshold and use a closing operator to fill small gaps. We create a map of the Euclidian distance to the nearest edge and group clusters of local maxima into single centers using a third nearest neighbor scan. We eliminate spurious maxima by requiring that the diameters of adjacent bubbles are larger than that of their joining face. A 3D Delauney triangulation from the center locations gives neighbors for each center. We estimate the averaged radius of the equivalent sphere for each center as the mean of the distances to all its neighbors.

The results are consistent with eqn. (7) with $\kappa = 1.0 \pm 0.3 \times 10^{-5}$ mm$^2$/sec and $f_0 = 12 \pm 2$ (fig. 2b). The constant offset from simulation and optical tomography data suggests that we have a systematic error in our volume estimate which causes us to overestimate the volume of large

bubbles. The large error bars primarily result from the approximations in determining the volumes. Because the wetness during imaging is similar, $\kappa$ is the same for the three samples we analyzed. We can thus combine the statistics from all three experiments. The errors stay roughly constant, suggesting that the averaged, not the exact, law holds.

## 7 Conclusions

Our current knowledge of 3D coarsening is inconsistent and fragmentary. We finally agree that the corrected growth rate of 3D grains depends only on their topology and not on their volume. However, some simulations (Potts, S.E. and vertex) suggest that the average growth rate for grains depends linearly on their number of sides while other simulations using the same models find a weakly nonlinear (approximately $f^{1/3}$) dependence. The experimental data favors the linear result but has such large error bars that it cannot rule out the nonlinear form. An ideal linear result would be intriguing since it is not mathematically necessary.

To determine whether the growth law holds for individual grains we need additional statistics from the S.E. simulations. We also need to reanalyze our MRI experiments which have excellent statistics but large errors in their volume estimates using the more accurate volume calculations of Monnereau *et al*. Faster scans and slower coarsening would increase the number of usable bubbles in each image and reduce selection bias. Investigating the growth rate as a function of detailed topology will determine if an exact law exists.

## Acknowledgements

## References

[1] J. von Neumann, *Metal Interfaces* (American Society for Metals, Cleveland, 1952) 108.
[2] J. A. Glazier, D. Weaire, J. Phys: Condens. Matter **4**, 1867 (1992).
[3] J. A. Glazier, *The Evolution of Cellular Patterns*, Ph.D. thesis, U. of Chicago, 1989.
[4] C. Monnereau, M. Vignes-Adler, J. Colloid and Interf. Sci. **202**, 45 (1998).
[5] C. Monnereau, M. Vignes-Adler Phys. Rev. Lett. **80**, 5228 (1998).
[6] B. Prause, *Magnetic Resonance Imaging Studies of Three-Dimensional Liquid Foams*, Ph.D. thesis, U. of Notre Dame, 2000.
[7] J. A. F. Plateau, *Statique Experiméntal et Théorique des Liquides Soumis aux Seules Forces Moléculaires* (Gauthier-Villars, Paris, 1873).
[8] W. W. Mullins, Acta Met. **37**, 2979 (1989).
[9] J. A. Glazier, Phys. Rev. Lett. **70**, 2170 (1993).
[10] J. E. Avron and D. Levine, Phys. Rev. Lett. **69**, 208 (1992).
[11] I. M. Lifschitz, V. V. Slyozov, Soviet J.E.T.P. **35**, 331 (1959).
[12] I. M. Lifschitz, V. V. Slyozov, J. Phys. Chem. Solids **19**, 35 (1961).
[13] W. W. Mullins, J. Viñals, Acta metall. **37**, 991 (1989).
[14] D. J. Durian, D. A. Weitz, D. J. Pine, J. Phys.: Condens. Matter **2**, SA433 (1990).
[15] D. J. Durian, D. A. Weitz, D. J. Pine, Science **252**, 686 (1991).
[16] F. Wakai, N. Enomoto, H. Ogawa, Acta mater. **48**, 1297 (2000).
[17] P. A. Mulheran, Phys. Rev. E **51**, R3803 (1995).

[18] S. A. Magrabi, B. Z. Dlugogorski, G. L. Jameson, Chem. Eng. Sci. **54**, 4007 (1999).

[19] H. V. Atkinson, Acta. Met. **36**, 469 (1988)

[20] N. Rivier, Philos. Mag. B **47**, L45 (1983).

[21] M. A. Fortes, J. Mat. Sci. **21**, 2509 (1986).

[22] C. Sire, Phys. Rev. Lett. **70**, 420 (1994).

[23] M. P. Anderson, G. S. Grest, D. J. Srolovitz, Scripta. Met. **19**, 225 (1985).

[24] G. Grest., D. Srolovitz, M. Anderson, Phys. Rev. B **38**, 4752 (1988).

[25] M. P. Anderson, G. S. Grest, D. J. Srolovitz, Phil. Mag. **B 59**, 293 (1989).

[26] D. Weaire, J. A. Glazier, Phil. Mag. Lett. **68**, 6 (1993).

[27] K. Fuchizaki, K. Kawasaki, Physica A **221**, 202 (1995).

[28] D. Weygand, Y. Bréchet, J. Lépinoux, W. Gust, Phil. Mag. B **79**, 703 (1999).

[29] C. Monnereau, M. Vignes-Adler, N. Pittet, Phil. Mag. B **79**, 1213 (1999).

[30] E. B. Matzke, Am. J. Bot. **26**, 288 (1939).

[31] E. B. Matzke, J. Nestler, Am. J. Bot. **33**, 130 (1946).

[32] P. L. White and L. H. van Vlack, Metallography **3**, 241 (1970).

[33] J. W. Marvin, Am. J. Bot. **26**, 280 (1939).

[34] E. T. Woodburn, L. G. Austin, J. B. Stockton, Trans. Inst. Chem. Eng. **72**, 211 (1994).

[35] P. D. Thomas, R. C. Darton, P. B. Whalley, Ind. Eng. Chem. Res. **37**, 710 (1998).

[36] R. M. Morris, A. Morris, Chem. and Ind. (November 13), 1902 (1965).

[37] P. D. Thomas, R. C. Darton, Chem. Eng. J. **56**, 187 (1995).

[38] J. B. German, M. J. McCarthy, J. Agric. Food Chem. **37**, 1321 (1989).

[39] B. A. Prause, J. A. Glazier, S. J. Gravina, C. D. Montemagno, J. Phys.: Condens. Matter **7**, L511 (1995).

[40] C. P. Gonatas, J. S. Leigh, A. G. Yodh, J. A. Glazier, B. Prause, Phys. Rev. Lett. **75**, 573 (1995).